INTERLAMINAR TOUGHENING OF CARBON FIBRE REINFORCED POLYMERS USING GRAPHENE / THERMOPLASTIC INSERTS

C. S. Nagi[1, 2*], S. L. Ogin[2], I. Mohagheghian[2], C. Crean[2] and A. D. Foreman[1]

[1]QinetiQ, Applied Science, Farnborough GU14 0LX, United Kingdom
Email: cnagi@qinetiq.com
[2] Faculties of Engineering and Physical Sciences, University of Surrey, Guildford GU2 7XH, United Kingdom

Keywords: Graphene, CFRP, Interlaminar toughening, Mechanical testing, Fracture analysis

Abstract

Carbon fibre reinforced polymer (CFRP) composites are used extensively in aerospace and automotive structural components. However, CFRP's are susceptible to impact damage which gives rise to phenomena such as delamination, in addition to matrix cracking and fibre fracture. Graphene's superior mechanical properties potentially make it an ideal material for improving the interlaminar properties of CFRP and thus enhancing delamination resistance. This paper presents preliminary work on enhancing the interlaminar toughness using a QinetiQ in-house manufacturing route whereby a thermoplastic insert material was modified with graphene additions, which produced graphene loadings of 0, 1 and 2 g/m^2 within the interlaminar region of CFRP samples. By measuring the fracture resistance of this interface, it has been found that an improvement in the mode-II performance occurred for a 1 g/m^2 addition, although the mode-I toughness was reduced. The largest improvement in fracture resistance was noted when the graphene loading was such that the graphene worked in tandem with existing toughening mechanisms. Conversely, a reduction in mechanical properties was largely due to excess quantities of graphene inhibiting these toughening mechanisms.

1. Introduction

Composite materials are widely used in various engineering applications, including structural components for aerospace and automotive applications. The lightweight, high strength and stiffness properties make them ideal for aerodynamic systems. In particular with aerospace structures, impacts from foreign objects, such as debris, hail or bird strike, can prove highly detrimental to the performance and integrity of the composite structure [1]. Through improving the toughness of CFRP, not only can impact damage be mitigated, but improvements to the efficiency of the structure may result in fuel savings.

Graphene is a 2D nanomaterial consisting of a single layer of carbon atoms arranged in a hexagonal lattice, shown to have a breaking strength of 130 GPa and a Young's modulus of 1 TPa [2]. Graphene can be functionalised to give rise to graphene oxide (GO), which contains carbonyl, epoxide and hydroxyl groups bonded to the basal plane of the graphene platelets [3]. Typical carbon to oxygen ratios can be anywhere between 1:1 to 10:1 for GO, versus 1000:1 for pristine single layer graphene [4]. The benefits of these groups is that they can be used to facilitate bonding to resins in dispersion, or as a filler material leading to lower weight fractions compared with other filler materials such as carbon nanotubes [5], while potentially achieving similar or improved properties.

Mechanical reinforcement of various resins by graphene [6] showed that to facilitate stress transfer, the minimum platelet diameter would be around 3 μm for pristine graphene and less than 1 μm for

GO. In terms of the platelet thickness, if the platelets are too thin then the cracks bow around the platelets reducing the beneficial effects of graphene. Therefore it has been suggested that the platelet thickness should be between 4 – 6 layers for optimal improvements in mechanical reinforcement.

Previous work (Ning et al. [7]), has shown that GO additions can improve the interlaminar toughness. In the work by Ning and colleagues, GO was dispersed into an epoxy resin and then the graphene oxide reinforced epoxy (GO-epoxy) was directly introduced at the interface. The epoxy resin for the GO-epoxy effectively acted as a carrier for GO to allow for transport into the CFRP while also assisting the dispersion of the GO.

In this paper, preliminary results are presented on introducing graphene into the interlaminar region of CFRP using a non-woven thermoplastic carrier with regard to toughness enhancements (i.e. mode-I and mode-II loading). This is part of a wider study on the effect of different graphene loadings on the toughness of the interlaminar region.

2. Materials and Method

2.1 Materials

Unidirectional CFRP pre-preg (MTC510 / T800) from SHD Composites was used to fabricate CFRP laminates; the carbon fibre diameter was 5 µm, and the volume content of resin was 34 wt. %. The graphene used for this study was A-GNP35 (Applied Graphene Materials). The as-received graphene was quoted by the manufacturer as having a platelet diameter of 3 – 120 µm and a thickness of 5 – 15 layers.

The graphene modified inserts were prepared using a non-woven thermoplastic modified with various loadings of graphene. A solvent dispersion of graphene was prepared to the desired concentration. Unidirectional CFRP laminates $[0°]_{16}$ were laid up with the graphene-modified interlayer inserted at the mid-plane along with a 12 µm release film to act as a crack initiator. The laminate was cured under pressure in an autoclave at 120±5 °C for 2 hours. To investigate the effects of various graphene loadings, the areal density of graphene-loaded thermoplastic interlayer was varied from 0 to 2 g/m^2. A total of 4 types of laminate were prepared: baseline (CFRP only), 0 (CFRP with a thermoplastic insert only), 1 and 2 g/m^2 (graphene-modified inserts).

2.2 Mechanical testing and fracture surface characterization

Mode-I and mode-II mechanical tests were carried out using Double Cantilever Beam (DCB) and End Notch Flexure (ENF) tests, respectively. The schematic in figure 1 shows the sample dimensions used for both mode-I and mode-II testing. Testing was carried out using an Instron 5500 in accordance with BS ISO 15024 [8] and ASTM D 7905 [9] for mode-I and mode-II tests, respectively.

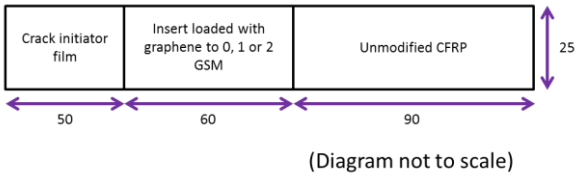

Figure 1: Typical geometry for 0, 1 and 2 g/m^2 mode-I and mode-II samples, with location of crack initiator film and toughening insert for mode-I and mode-II samples. (Baseline samples do not contain the 60mm insert after the crack initiator film).

A schematic of the mode-I test arrangement is shown in figure 2(a); the crosshead speed was 1 mm/min. The length of crack initiator film was 40 mm and the crack was grown to a minimum length of 35 mm from the end of the crack initiator film. On processing of the load versus displacement data, a crack growth length of 35 mm was used to ensure that the crack tip only interacted with the graphene modified region.

A schematic of the mode-II tests is shown in figure 2(b); here the crosshead displacement was 2 mm/min. Each test had a pre-cracking stage (to initiate a sharp, well defined crack tip), followed by a fast fracture stage where the crack grew unstably. The *a/L* ratio was adjusted to 0.8 and 0.5 for pre-crack and fast fractures stages, respectively, where *a* is the initial crack length and *L* is the half span length. The applied load and crosshead displacement were recorded during the tests. As the half span length is equal to 50 mm then the crack length to satisfy the pre-crack and fast fracture criteria are 40 and 25 mm, respectively. After both mode-I and mode-II tests, the fracture surfaces of the test samples were carefully separated and examined using either a Hitachi S-3200N or JEOL JSM-7100F scanning electron microscope. The accelerating voltage was set to 10 kV, the working distance set at 15 to 20 mm, and a tilt of 15 – 20° was used to highlight the fracture surface topography.

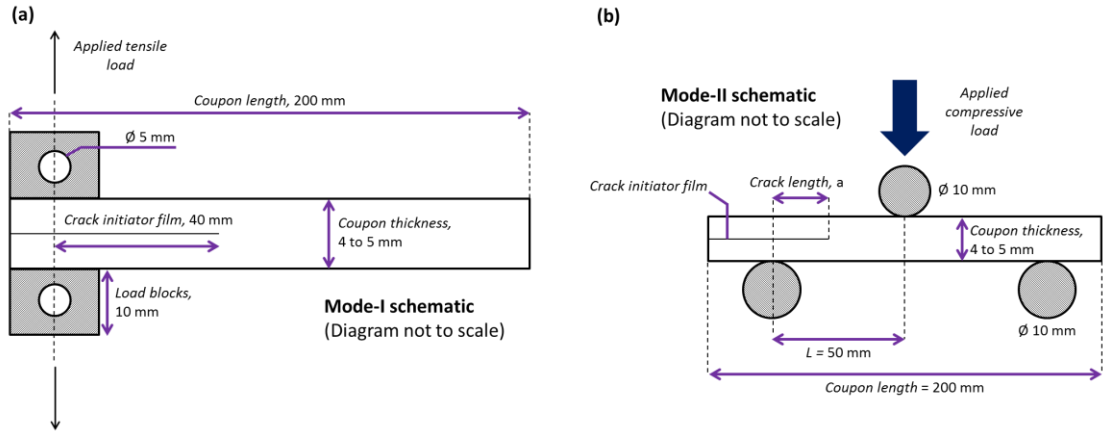

Figure 2: Schematic showing mode-I (a) and mode-II (b) test setup.

3. Results

3.1 Mode-I loading

Typical mode-I load against displacement curves are shown in figure 3. The load initially increases approximately linearly with the displacement until crack initiation and propagation occurs. Variations in the initial slope, prior to the peak load, are believed to be due to small differences in the length of the crack initiator film. The baseline materials showed a peak at the initiation value followed by a drop in the load which was probably due to the resin fillet region. This was followed by a relatively linear drop in load with crosshead displacement, indicating stable crack growth. The 0 g/m^2 samples showed an initial peak load followed by saw-tooth behaviour, and then stable crack growth with a gradual reduction in load, characteristic of R-curve behavior and significant fibre bridging. By contrast, the 1 g/m^2 and 2 g/m^2 show quite different behavior once the crack initiates, with a sharp reduction in load with increasing displacement. For a loading of 2 g/m^2 it was particularly noticeable that the crack grew unstably; the crack rapidly grew a few millimeters at a time, with periods of crack arrest. Table 1 shows the average G_{1C} propagation values.

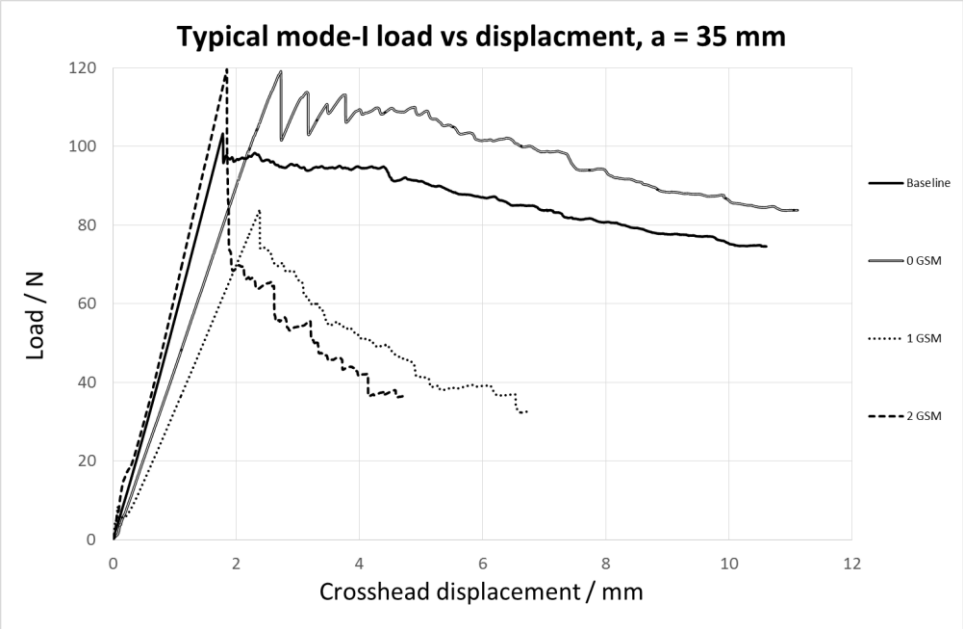

Figure 3: Typical mode-I load vs displacement graphs for (a) baseline material, (b) 0 g/m^2, (c) 1 g/m^2 and (d) 2 g/m^2 samples.

Table 1: Table showing mode-I load, displacement and G_{1C} values.

Graphene loading (g/m^2)	*Avg. $G_{1C\ (prop)}$ values* (J.m^{-2})	*% change versus baseline*
Baseline CFRP	530	N/A
0	582	+10 %
1	214	-60 %
2	157	-70 %

A photograph taken during the test for a 2 g/m^2 sample is shown in figure 4(a). Its corresponding R-curve is presented in figure 4(b) showing the G_{1c} values for different crack lengths. In the region of the graphene loaded insert, no fibre bridging was visible (Fig. 4 (a)) and which corresponds to the low mode-I value (Fig. 4(b)). In this example, the crack was grown further than the initial 35 mm test and into the unmodified region of the sample, where there was no insert. Beyond the region of the graphene-modified insert, fibre bridging can be seen, corresponding to an increase in G_{1c}.

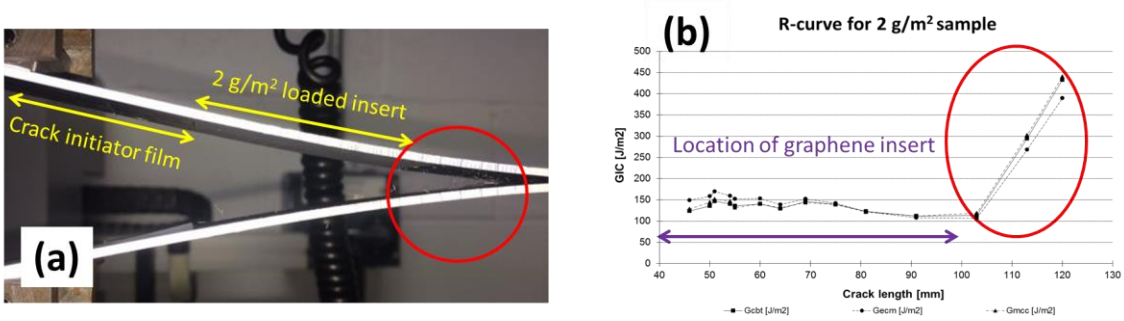

Figure 4: (a) 2 g/m^2 sample on test, showing fibre bridging; (b) the corresponding R-curve data.

Figure 5, shows SEM images of the crack growth region after approximately 10 mm of crack growth for all specimen types. For the baseline materials and the 0 g/m^2 (Fig. 5(a) + (b)), the primary toughening mechanism appears to be the fibre bridging from the CFRP with toughening contributions from the thermoplastic insert for the 0 g/m^2 samples, highlighted by the dashed circle (Fig. 5(b)). At the graphene loading of 1 g/m^2 (Fig. 5(c)), some indication of fibre bridging having occurred was observed as fibre imprints shown by the grooves in the graphene modified resin, although this is considerably less than in the baseline material. At 2 g/m^2 (Fig. 5(d)), there are now no traces of fibre imprints in the fracture surface, suggesting that fibre bridging is no longer occuring; with this high graphene loading, the interlaminar region now appears to consist of a continuous layer of resin-loaded graphene along the plane of fracture.

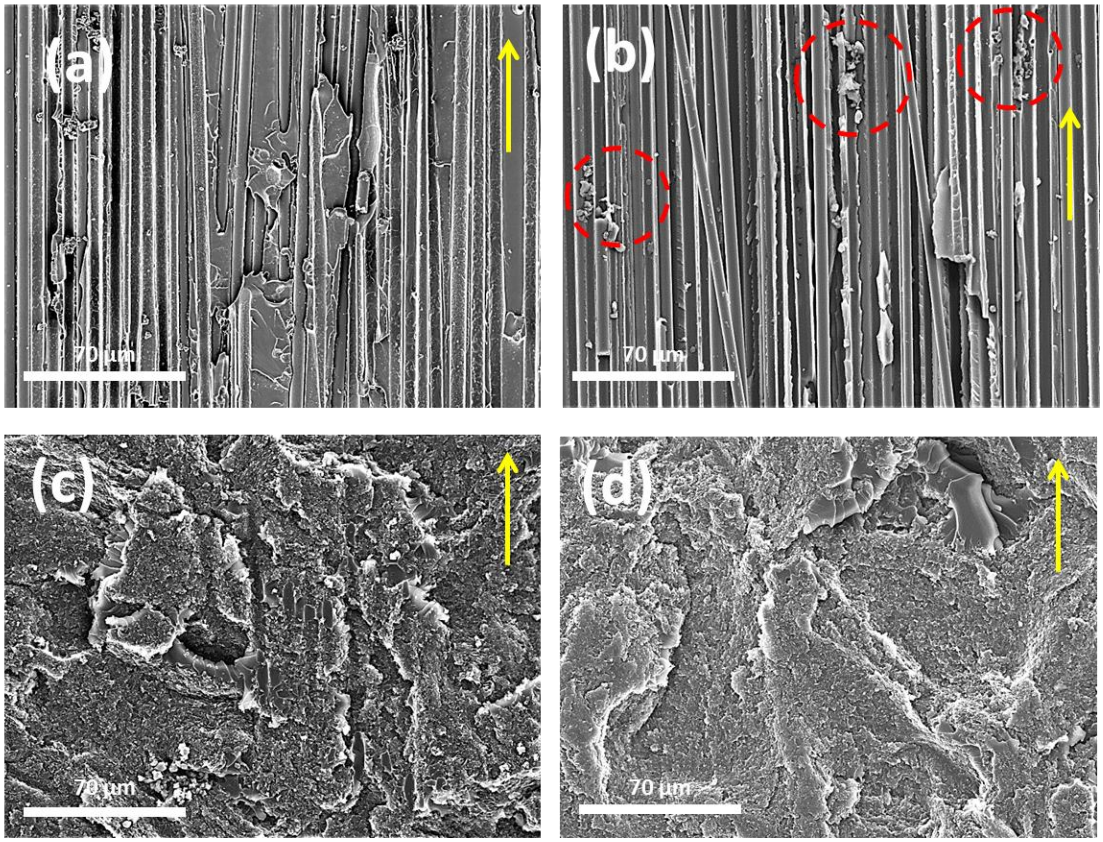

Figure 5: SEM micrographs showing mode-I fracture surface for (a) baseline material, (b) 0 g/m^2, (c) 1 g/m^2, and (d) 2 g/m^2 samples.

3.2 Mode-II loading

Typical mode-II load versus displacement graphs are shown in figure 6. The initial slope of the curves varies slightly due to the positioning of the centre roller once the pre-crack has been established. For the baseline material and for 0 g/m^2 (i.e. thermoplastic insert only, 0 g/m^2), the load increases linearly with displacement up to the point where crack growth begins. The drop in load coincides with the crack growing in a semi-stable manner, instead of the expected unstable crack growth of fast fracture. At 0 g/m^2, the thermoplastic insert provided a toughening contribution, shown by the higher peak load compared to the baseline material. For the 1 g/m^2 and 2 g/m^2 samples, after attaining the maximum load, unstable fast-fracture occurred. Overall, the 1 g/m^2 samples showed the highest value of G_{IIC}, showing an increase of +92 % from the baseline material (Table 2).

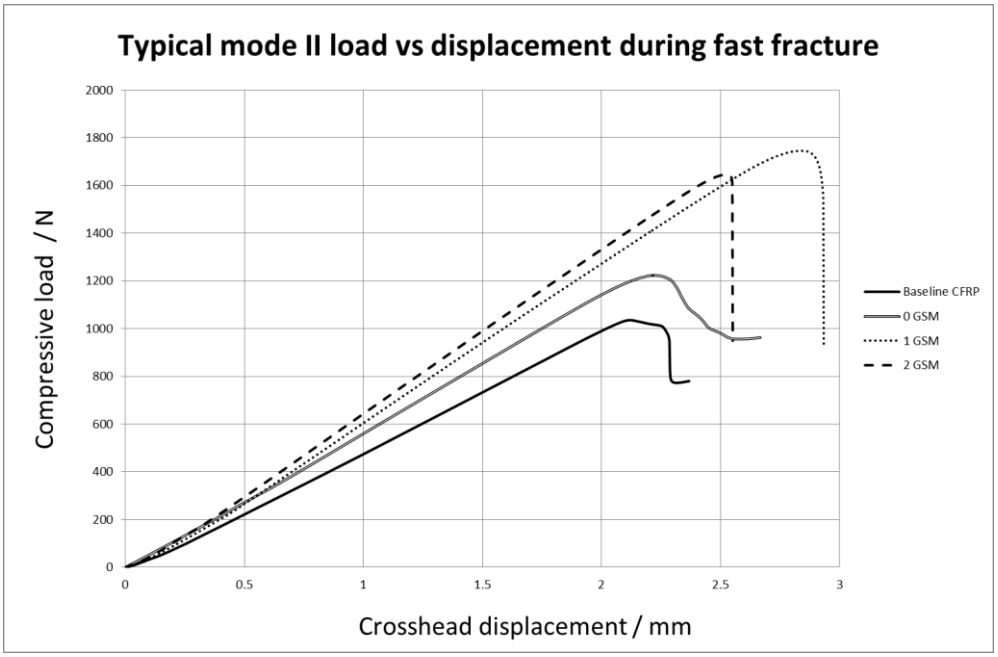

Figure 6: Typical mode-II load vs displacement graphs for (a) baseline material, (b) 0 g/m^2, (c) 1 g/m^2, and (d) 2 g/m^2 samples.

Table 2: Table showing mode-II load versus displacement and G_{2C} values.

Graphene loading (g/m^2)	*Avg. G_{IIC}* (J.m^{-2})	*% change versus baseline*
Baseline CFRP	961	N/A
0	1 086	+13 %
1	1 904	+92 %
2	1 550	+61 %

The fracture surfaces for the baseline material and the 0 g/m^2 material are shown in figures 7(a) and 7(b), respectively. In both cases, the formation of shear cusps at 45° within the resin with respect to the crack growth direction are visible which is evidence of the surface failing in shear. This is believed to be the primary toughening mechanism. At 1 g/m^2 (Fig. 7(c)), shear cusps are still visible, though much of the crack path appears to be through the resin loaded with graphene. At 2 g/m^2 (Fig. 7(d)), a higher percentage of the fracture surface appears to be the resin-loaded graphene, with little evidence of shear cusps.

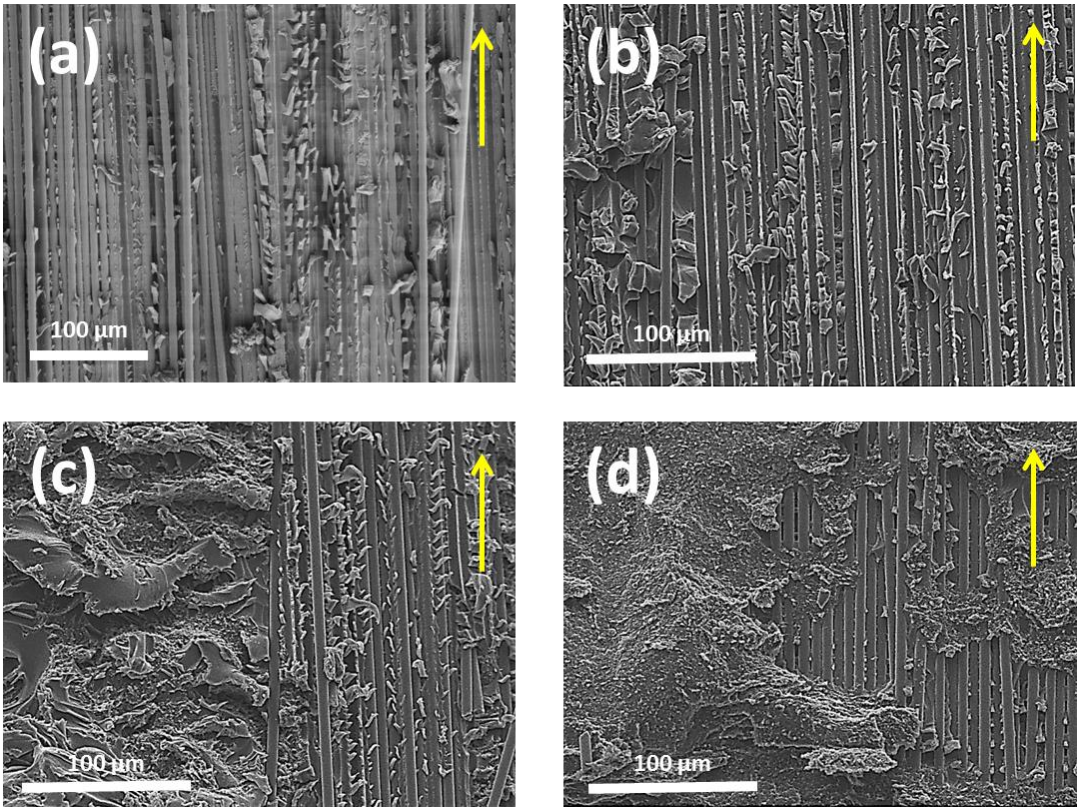

Figure 7: SEM micrographs showing mode-II fracutre surface for (a) baseline material, (b) 0 g/m^2, (c) 1 g/m^2, and (d) 2 g/m^2 samples. The arrow indicates the crack propagation direction.

5. Concluding remarks

A graphene-modified thermoplastic insert has been used to introduce graphene into the interlaminar region of a CFRP laminate. For all graphene additions investigated, the addition of graphene in this manner had an adverse effect on the mode-I toughening, primarily due to the graphene preventing fibre bridging from occurring. However, under mode-II conditions an increase of +92 % in toughness was noted at 1 g/m^2. It can be concluded that high graphene loadings using the current manufacturing technique can cause resin-loaded graphene aggregate formation in the interlaminar region which leads to the inhibition of other toughening mechanisms. Further work is proceeding using lower graphene additions.

Acknowledgments

This research is supported by the EPSRC (award no. EP/G037388). The authors would like to acknowledge the support received from the Composites Team of the Materials Group at QinetiQ (Farnborough) and the Microstructural Studies Unit (MSSU) at the University of Surrey. In conjunction with, Applied Graphene Materials (AGM) for graphene materials support and the National Composites Centre (NCC) for the processing of CFRP laminates.

References

[1] S. Agrawal, K. K.Singh, & P.K. Sarkar. Impact damage on fibre-reinforced polymer matrix composite–a review. *Journal of Composite Materials*, *48*(3), 317-332, 2014

[2] C. Lee, X. Wei, J. W. Kysar, & J. Hone. Measurement of the elastic properties and intrinsic strength of monolayer graphene. *Science*, *321*(5887), 385-388, 2008.
[3] W. Gao. The chemistry of graphene oxide. *Springer, Cham*, 61-95, 2015.
[4] A. A. King, B. R. Davies, N. Noorbehesht, P. Newman, T. L. Church, A. T. Harris, ... & A. I. Minett. A new Raman metric for the characterisation of graphene oxide and its derivatives. *Scientific reports*, *6*, 19491, 2016.
[5] G. Mittal, V. Dhand, K. Y. Rhee, S. J. Park, & W. R. Lee. A review on carbon nanotubes and graphene as fillers in reinforced polymer nanocomposites. *Journal of Industrial and Engineering Chemistry*, 21, 11-25, 2015.
[6] R. J. Young, I. A. Kinloch, L. Gong, & K. S. Novoselov. The mechanics of graphene nanocomposites: a review. *Composites Science and Technology*, *72*(12), 1459-1476, 2012.
[7] H. Ning, J. Li, N. Hu, C. Yan, Y. Liu, L. Wu, ... & J. Zhang. Interlaminar mechanical properties of carbon fiber reinforced plastic laminates modified with graphene oxide interleaf. *Carbon*, *91*, 224-233, 2015.
[8] BS ISO 15024, Fibre-reinforced plastic composites–determination of mode I interlaminar fracture toughness, HIC for unidirectionally reinforced materials. *British Standards International*. 2001.
[9] ASTM D 7905, Standard Test Method for Determination of the Mode II Interlaminar Fracture Toughness of Unidirectional Fiber-Reinforced Polymer Matrix Composites, Vol. 1. No. Reapproved, *ASTM International*, 1-18, 2014.